

Catalysis Science & Technology

Accepted Manuscript

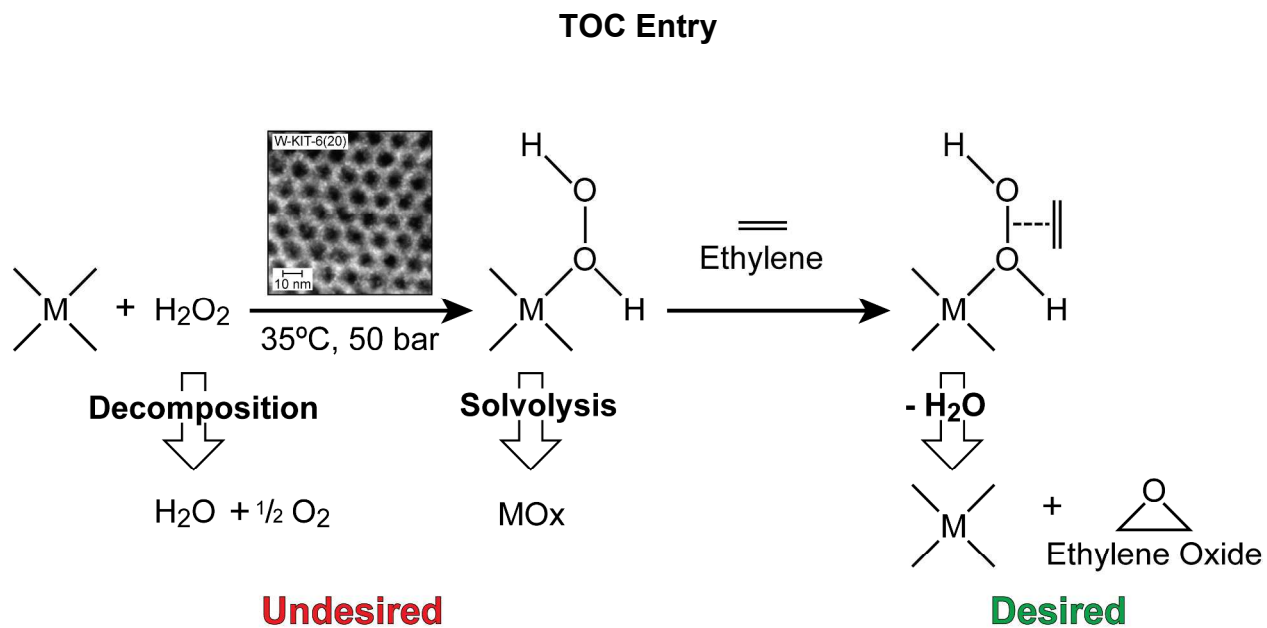


This is an *Accepted Manuscript*, which has been through the Royal Society of Chemistry peer review process and has been accepted for publication.

Accepted Manuscripts are published online shortly after acceptance, before technical editing, formatting and proof reading. Using this free service, authors can make their results available to the community, in citable form, before we publish the edited article. We will replace this *Accepted Manuscript* with the edited and formatted *Advance Article* as soon as it is available.

You can find more information about *Accepted Manuscripts* in the [Information for Authors](#).

Please note that technical editing may introduce minor changes to the text and/or graphics, which may alter content. The journal's standard [Terms & Conditions](#) and the [Ethical guidelines](#) still apply. In no event shall the Royal Society of Chemistry be held responsible for any errors or omissions in this *Accepted Manuscript* or any consequences arising from the use of any information it contains.



Nb- and W-KIT-6 materials display significant ethylene epoxidation activity with H_2O_2 as oxidant at mild temperatures that eliminate substrate burning.

Towards Highly Selective Ethylene Epoxidation Catalysts Using Hydrogen Peroxide and Tungsten- and Niobium-Incorporated Mesoporous Silicate (KIT-6)

Wenjuan Yan^{1,2}, Anand Ramanathan¹, Madhav Ghanta,^{1,2,3} Bala Subramaniam^{1,2*}

¹Center for Environmentally Beneficial Catalysis, Lawrence, Kansas 66047.

²Department of Chemical and Petroleum Engineering, University of Kansas, Lawrence, KS 66045

³Currently with SABIC Innovative Plastics, Selkirk, NY 12158.

*To whom correspondence should be addressed. E-mail: bsubramaniam@ku.edu; Phone: 785-864-2903; Fax: 785-884-6051

ABSTRACT

Significant ethylene epoxidation activity was observed over Nb- and W- incorporated KIT-6 materials with aqueous hydrogen peroxide (H₂O₂) as oxidant and methanol as solvent at mild operating conditions (35 °C and 50 bars) where CO₂ formation is avoided. The Nb-KIT-6 materials generally show greater epoxidation activity compared to the W-KIT-6 materials. Further, the ethylene oxide (EO) productivity observed with these materials [30-800 mg EO/h/(g metal)] is of the same order of magnitude as the conventional silver (Ag) based gas phase ethylene epoxidation process. Our results reveal that the framework-incorporated metal species, rather than the extra framework metal oxide species, are mainly responsible for the observed epoxidation activity. However, the tetrahedrally coordinated framework metal species also introduce Lewis acidity that promotes their solvolysis (that results in the framework metal

species also being gradually leached) as well as H₂O₂ decomposition. These results and mechanistic insights provide rational guidance for developing catalysts with improved leaching resistance and minimal H₂O₂ decomposition.

KEYWORDS: Epoxidation, ethylene, ethylene oxide, niobium, tungsten, KIT-6.

1. Introduction

Ethylene oxide (EO) is one of the widely used chemical intermediates, with applications in the production of detergents, thickeners, solvents, plastics and various organic chemicals. In 2013, the global EO production capacity was approximately 20.5 million metric tons. During the next decade, the EO demand is projected to grow at an annual rate of 6-7%.¹ Currently, EO is produced through vapor phase ethylene epoxidation over Ag-based catalysts using O₂ as oxidant. A major challenge in this technology has been to curtail the burning of ethylene as well the EO to CO₂ at typical reaction temperatures (200-240°C). To reduce burning, promoters such as Cs, Cd, Cu and Pt have been added to the Ag catalyst.²⁻⁴ Such catalyst modifications have resulted in remarkable enhancements in EO selectivity, from 45% in 1945 to approximately 90% at present. Despite these improvements, the CO₂ released as byproduct is still approximately 3.4 million metric tons per year, making it the second largest emitter of CO₂ among all chemical process after ammonia synthesis. Further, the ethylene burning alone translates to a monetary loss of approximately \$1.6 billion/year assuming an ethylene price of 32¢/lb.⁵

With the increased availability of ethane as a collateral product from shale gas recovery, alternate EO technologies that better conserve ethylene feedstock have assumed renewed importance. Recently, we reported a liquid phase ethylene epoxidation process (also referred

herein as the CEBC process) that eliminates ethylene burning and produces EO with nearly total selectivity.^{1,6,7} At mild operating conditions of 40 °C and 50 bar, the catalyst (methyltrioxorhenium, MTO) shows high activity (1,610-4,970 mg EO/h/g Re) with the H₂O₂ fully utilized toward EO formation.¹ The oxidant (H₂O₂), operating conditions (20-40°C, 50 bar) and solvent (methanol) are very similar to those employed in the Dow-BASF HPPO technology for making propylene oxide.⁸ The main difference is that the HPPO process uses a heterogeneous TS-1 catalyst that does not work for ethylene epoxidation. Preliminary economic analysis suggests that the Re-based EO process has the potential to be competitive if the Re recycle is nearly quantitative.⁷ The EO production cost via the conventional Ag-catalyzed process (that uses O₂ as oxidant) is estimated to be 58¢/lb. The corresponding EO production cost via the MTO-catalyzed process (that uses H₂O₂ as oxidant) is 57¢/lb, when assuming a catalyst life of 1 year and a leaching rate of 0.11 lb MTO/h. The costs of the oxidant (H₂O₂) and catalyst (Re-based) in the CEBC are significantly higher than their counterparts (O₂ and Ag, respectively) in the conventional process. However, the higher oxidant and catalyst costs are offset by gains made in other operating costs stemming from more effective ethylene utilization in the CEBC process. Yet, the performance metrics (on catalyst life, activity and maximum catalyst leaching rate) for practical viability of the CEBC process are rather demanding. This aspect, coupled with the low abundance and high cost of Re metal (\$1,400/lb), poses significant challenges for the commercialization of any Re-based technology and prompted us to investigate alternative ethylene epoxidation catalysts that are relatively inexpensive and heterogeneous in nature.

In this context, W and Nb modified heterogeneous catalysts on MCM-41 and SBA-15 type supports have been shown to exhibit excellent catalytic activities for epoxidation of cyclohexene,⁹⁻¹¹ cyclooctene,^{9,12-14} and methyl oleate.^{15,16} However, two of the important

performance measures, viz., the stability of H_2O_2 against decomposition and metal leaching from the catalysts have not been clearly addressed in the referenced papers. In the present work, we have synthesized and evaluated W¹⁷ and Nb¹⁸ incorporated mesoporous materials for ethylene epoxidation with H_2O_2 as oxidant under mild conditions (35 °C and 50 bar).¹⁹ We chose silica-based cubic mesoporous supports (KIT-6, KIT-5) that have attracted much attention in recent years due to their high surface area and uniform pore size.^{20,21} In evaluating the performance of these catalysts, we investigated metal leaching and H_2O_2 stability, critical aspects to establish practical viability. The W-KIT-6 and Nb-KIT-6 catalysts are shown to be active for ethylene epoxidation at mild conditions. However, significant H_2O_2 decomposition and metal leaching from the catalyst were observed. Plausible mechanisms for both epoxidation and catalyst deactivation are proposed with a view to rationally developing improved catalysts that display near-quantitative EO selectivity while also thwarting H_2O_2 decomposition and metal leaching.

2. Experimental

2.1 Materials

Methanol (MeOH), employed as solvent, was used as received without further purification. Ceric sulfate (0.1 N) and trace metal grade sulfuric acid (99.9 wt. %) were purchased from Fischer Scientific. Ethylene (high purity grade) was purchased from Matheson Tri-Gas Co. The oxidant (50 wt% H_2O_2 in H_2O), ferroin indicator solution, acetonitrile (AN) (HPLC grade 99.9 wt.% purity), anhydrous ethylene glycol (EG), and tungsten (VI) oxide (WO_3) powder, 99.995 wt.% purity) were purchased from Sigma-Aldrich and used without further purification. The EO standard was purchased from Supelco Analytical.

2.2 Catalyst synthesis and characterization

Mesoporous W-KIT-6 and Nb-KIT-6 catalytic materials used in this study were synthesized and characterized in detail, as reported elsewhere.^{17,18}

2.3 Silylation of Nb-KIT-6 using hexamethyldisilazane (HMDS)

In a typical silylation procedure, 2 g of Nb-KIT-6 (Si/Nb = 40) was heated to 120 °C under vacuum for 12 h. The calcined material was then dispersed in 30 mL of a 5 wt.% solution of HMDS in dry toluene. The dispersion was stirred for 7 h at 120 °C. The resulting solid was filtered and washed with 100 mL of dry toluene and 200 mL of anhydrous ethanol. This process was repeated thrice.

2.4 Catalytic epoxidation studies

The schematic of the reactor setup is shown in Figure S1 (ESI). The reactor and the operating procedure have been described previously.¹ Briefly, the catalysts were tested for ethylene epoxidation in a 50 mL Parr reactor operated at 35 °C, 50 bar and at 1400 rpm (to eliminate gas-liquid mass transfer limitations). At these conditions, ethylene ($P_c = 50.6 \pm 0.5$ bar, $T_c = 9.3 \pm 0.5$ °C) is near its critical point and hence exhibits liquid-like density, causing it to substantially dissolve in the liquid phase, expanding its volume by up to 15%.¹ Thus, the reaction occurs in an ethylene-expanded liquid phase. Prior to reaction, the catalyst samples were activated in a stream of flowing air at 500 °C for 5 h with a heating rate of 2°C/min. A solution containing 50 wt.% H₂O₂/H₂O solution (118 mmol H₂O₂), MeOH (624 mmol) and acetonitrile (AN) as internal standard (4.9 mmol) was charged into the Parr reactor. Isothermal, constant-pressure, batch reactions lasting up to 5 h were performed with each catalyst sample. The reaction mixture was sampled at regular intervals to determine the concentrations of the desired product (EO) and the by-products [ethylene glycol (EG) and 2-methoxyethanol (2-ME)]. A Hewlett-Packard 5890

Series II gas chromatograph (GC) employing a CP-WAX 58 (FFAP) CB capillary column (25 m x 0.25 mm x 0.2 μ m), equipped with a flame ionization detector, was used for the analysis of the liquid phase. Figure S2 (ESI) shows a sample chromatogram with well-resolved GC/FID peaks for ethylene, EO, MeOH, AN, 2-ME and EG. The H₂O₂ concentration in the reaction mixture, before and after reaction, was determined by redox titration with ceric (IV) sulfate and ferroin indicator. Both the fresh and used catalysts were digested with HF and H₂SO₄ in an autoclave at 100°C for up to 5 h, and the resulting solution was used for performing elemental analysis by ICP-OES technique.

The following definitions are used in assessing the performance of the tested catalysts.

$$\text{TOF} = \frac{m_{EO}}{(\text{batch time})(m_{\text{metal}})}$$

$$S_{EO} = \left(\frac{n_{EO}}{n_{EO} + n_{2-ME} + n_{EG}} \right) \times 100\%$$

$$U_{H_2O_2} = \frac{n_{EO} + n_{2-ME} + n_{EG}}{n_{H_2O_2}^0 - n_{H_2O_2}} \times 100\%$$

$$X_{H_2O_2} = \frac{n_{H_2O_2}^0 - n_{H_2O_2}}{n_{H_2O_2}^0} \times 100\%$$

where TOF, S_{EO} , $U_{H_2O_2}$, and $X_{H_2O_2}$ denote EO productivity (mg EO/h/g metal), EO selectivity, H₂O₂ utilization toward EO formation (also defined as the H₂O₂ utilization efficiency) and H₂O₂ conversion, respectively;

m_{EO} and n_{EO} represent the mass of EO formed and the mass of metal in the catalyst, respectively.

n_{EO} , n_{2-ME} and n_{EG} denote the molar amounts of EO, 2-ME and EG formed, respectively.

$n_{H_2O_2}^o$ and $n_{H_2O_2}$ denote the initial and the final molar amounts of H_2O_2 , respectively. As shown in Tables 2 and 3, the uncertainty in the measured values of the various performance metrics, established through repeated runs, is within 3% of the reported mean values.

3. Results and discussion

3.1 Catalyst Characterization

Detailed physicochemical characterizations of the catalyst samples may be found elsewhere.^{17,18} Only the salient features are summarized here. The mesoporous nature of W and Nb catalyst samples was confirmed by small angle X-ray scattering and N_2 sorption studies. The physicochemical characteristics are summarized in Table 1. For all the samples, the surface area ranges from 625-997 $m^2 g^{-1}$, decreasing at increased metal loadings (1.5-17.9 wt.%). In general, Nb-KIT-6 materials display larger pore diameter (8.5 nm) and lower acidity (0.11-0.34 mmol $NH_3 g^{-1}$) compared to W-KIT-6 (6.4-6.9 nm and 0.26-0.46 mmol $NH_3 g^{-1}$). Diffuse reflectance UV-Vis characterizations reveal that W is incorporated in the catalyst in at least three forms as follows: isolated tetrahedrally coordinated WO_4 (~206 nm), nanoparticles of WO_3 (~270 nm) and bulk WO_3 (~420 nm, observed only at higher W loadings).¹⁷ In contrast, for Nb-KIT-6, only the absorption peak due to isolated framework incorporated NbO_4 was noticed at 195 nm. Even at the highest Nb loading, no absorption bands around 320-340 nm, characteristic of Nb_2O_5 species, are evident. However, the bands at 220 and 270 nm suggest that oligomeric NbO_4 units are present in all samples even at low Nb loadings.¹⁸

3.2 Catalyst performance for ethylene epoxidation

3.2.1 Intrinsic activity

W-KIT-6 and Nb-KIT-6 catalysts were tested to compare EO productivity, EO selectivity, H₂O₂ utilization for EO formation and metal leaching. The results are summarized in Table 2. The support material, Si-KIT-6, showed negligible EO formation. However, under similar operating conditions, the W- and Nb- incorporated KIT-6 materials are active for ethylene epoxidation. The TOF observed with W-KIT-6 (34-152 mg EO/h/g W) and Nb-KIT-6 (234-794 mg EO/h/g Nb) catalysts are at the lower end of the activity reported for conventional Ag catalysts (700-4,400 mg EO/h/g Ag).²² The initial epoxidation rate (R_{EO}) estimated from the slope of the temporal formation profile at early time, was used to quantitatively assess the significance of gas-liquid (α_1), liquid-solid (α_2) and intraparticle mass transfer resistances (ϕ), employing established criteria (Table 4).^{23,24} The estimated values of α_1 , α_2 and ϕ are $1.83 (10^{-4})$, $3 (10^{-13})$ and $9.5(10^{-14})$, respectively, indicating that both external and intraparticle mass transfer limitations are insignificant at the investigated conditions. Details of estimating these parameters are presented in Tables S1 and S2 (ESI).

As inferred from Table 2 (entries 1-4), the TOF generally decreased with an increase in W content. For example, the TOF decreased from 152.6 to 34.4 mg EO/h/(g W), as the W loading was increased from 2.2 to 17.9 wt%. A similar trend was also observed with Nb-KIT-6 catalysts (Table 2, entries 5-8). These results might suggest that the extra-framework oxide species observed at higher metal loadings may not be active for epoxidation. Indeed, negligible EO was formed when WO₃, H₂WO₄, Na₂WO₄ (see Table 2, entries 9, 10 and 11), Nb₂O₅ and niobium oxalate (see Table 2, entries 12 and 13) were tested under similar operating conditions.

Even though all the tested catalysts show activity for ethylene epoxidation, the H_2O_2 utilization efficiency ($U_{\text{H}_2\text{O}_2}$) ranges from 1.8-18.8 % (Table 2) and is thus low. In the absence of ethylene, the H_2O_2 conversion under otherwise similar operating conditions was 14.1% (Table 2, entry 23) even on Nb-KIT-6, which shows the highest H_2O_2 utilization efficiency for EO formation (~18%). However, no detectable H_2O_2 decomposition was observed with just the support material (Si-KIT-6), during a run without substrate (ethylene) at similar operating conditions (Table 2, entry 22). This suggests that the acidity imparted by metal incorporation into the KIT-6 support (see Table 1) is a causative factor for H_2O_2 decomposition.

The effect of temperature on EO productivity was investigated with the Nb-KIT-6 catalyst that showed the highest activity (Si/Nb = 20). As inferred from Table 5, whereas increasing the temperature from 35-50 °C has little effect on the TOF, the EO selectivity decreased significantly from 76.3 to 38.2 % as side reactions begin to dominate. In addition, enhanced H_2O_2 conversion ($X_{\text{H}_2\text{O}_2}$) but lower H_2O_2 utilization efficiency ($U_{\text{H}_2\text{O}_2}$) was noticed at the higher temperatures.

Figure 1 shows the temporal variations in the formation of EO and other liquid phase products (EG and 2-ME) over Nb-KIT-6 (Si/Nb = 20) at 35°C. Clearly, the EO selectivity decreases with time due to several parallel adverse events, including reaction of the EO to form side products (such as EG and 2-ME), metal leaching and H_2O_2 decomposition. It is known that the presence of water blocks Lewis acid sites and forms Brønsted acid sites.¹⁰ While Lewis acidity enhances ethylene conversion and stabilizes the epoxide, Brønsted acid sites are known to favor the ring opening of chemisorbed epoxide to form the glycol.²⁵ As shown in Figure 2, the EO selectivity decreases significantly over Nb-KIT-6 catalysts as the number of Brønsted acid sites increases.¹⁸

3.2.2 Catalyst/H₂O₂ stability

Recycle tests were carried out with selected catalyst samples for up to two cycles. Following the initial run with the fresh catalyst, the recovered solids were calcined in air at 500°C for 5 h and reused. As summarized in Table 3, ICP-OES analysis of the spent reaction mixture revealed that 32~75% of the metal in the catalyst had leached out during the first 5 h run. Interestingly, as shown in Table 2 (entries 14-19), the TOF of the recycled W-KIT-6 and Nb-KIT-6 catalysts increased during the second 5 h run with the recovered catalysts from the first run. This suggests that inactive metal species (such as the oxides) initially leach out. However, as seen with the W-KIT-6 samples, the framework-incorporated metal species also leach out in subsequent recycles resulting in a TOF decrease during the second recycle run (Table 2, entry 15), eventually causing complete catalyst deactivation. Similar leaching was reported from heterogeneous catalysts based on Mo, W, Cr, V and Ti,^{26,27,28} in the presence of either H₂O₂ alone or H₂O₂ along with the substrate. In our experiments, we also observe substantial leaching of tungsten species during a blank experiment with only H₂O₂ and without methanol or ethylene (Table 3, entry 13). Further, we observe reduced tungsten leaching (24% in 5 h) during a blank run with only the solvent (Table 3, entry 12). In this case, we suspect that the extraframework oxide species, rather than framework metal species, are being primarily leached.

In addition to metal leaching, we also observe H₂O₂ decomposition on the M-KIT-6 catalysts. Interestingly, our experimental results (entries 22 and 23, Table 2) unambiguously show that H₂O₂ is stable on KIT-6 support (with either low or no measurable acidity) suggesting that the significant acidity measured on M-KIT-6 materials causes H₂O₂ decomposition.

Based on the foregoing observations, we postulate the following mechanism for the epoxidation, metal leaching and H_2O_2 decomposition over M-KIT-6 catalysts (Scheme 1). The tetrahedrally coordinated metal in the KIT-6 matrix forms a metal peroxo complex by reaction with H_2O_2 . Experimental evidence for such complex formation on W-grafted MCM-41 material has been previously reported.²⁹ It is also commonly known that such peroxo species easily undergo reaction with olefinic substrates to form the corresponding epoxide. The peroxo species may either undergo reaction with ethylene leading to the formation of ethylene oxide or undergo solvolysis resulting in the formation of inactive metal oxide species that are easily leached. As shown in Scheme 1, H_2O_2 also undergoes parallel decomposition. Our experimental results indicate that both these deactivation pathways (involving the metal peroxo species and H_2O_2 decomposition) stem from the acidity of the M-KIT-6 materials due to metal incorporation. These mechanistic insights therefore suggest that reducing the acidity could minimize, if not eliminate, these adverse side reactions.

3.2.3 Performance of silylated catalysts

Silylation, involving the substitution of $-\text{OH}$ groups on the catalyst surface by $-\text{OSiR}_3$ groups, has been shown to reduce acidity and H_2O_2 decomposition.³⁰ In addition, silylation is also reported to make the catalyst pores more hydrophobic, thereby excluding water.³¹ In an effort to reduce the undesired side reactions, a fresh batch of Nb-KIT-6 (Nb/Si = 40) was silylated according to reported procedure³² and tested for ethylene epoxidation. As summarized in Table 2 (entries 20-21), it was found that the silylated catalysts display higher EO selectivity even though the EO yield is lower than the calcined catalysts under similar operating conditions. The corresponding H_2O_2 conversion ($X_{\text{H}_2\text{O}_2}$) in the silylated catalyst was roughly a third of that

observed on the calcined catalyst with slightly higher H_2O_2 utilization efficiency ($U_{\text{H}_2\text{O}_2} = 5.3 \%$). It seems plausible that some of the active metal sites in the catalyst are blocked by the long chain $-\text{OSiR}_3$ groups. Further, based on ICP-OES analysis, approximately 25% of the Nb metal leached out of the silylated catalysts after 5 h, which is slightly less than the leaching observed with the calcined but unsilylated catalysts (36% Nb leaching under similar reaction conditions, Table 3, entries 9 and 10). Furthermore, ICP-OES analysis of the spent reaction mixture indicates the leaching of Si (~9%) as well, which was not observed when unsilylated M-KIT-6 catalysts were used. This clearly indicates that the $-\text{OSiR}_3$ groups themselves are also being gradually leached. Thus, while silylation techniques partially reduce metal leaching and H_2O_2 decomposition, alternate passivation techniques are required to thwart metal leaching and enhance H_2O_2 utilization. We are currently investigating the use of lower metal loadings (to lower acidity) in conjunction with the use of base pretreatment to reduce the acidity of the catalysts and thereby improve the H_2O_2 utilization efficiency.

4. Conclusions

W-KIT-6 and Nb-KIT-6 materials are shown to epoxidize ethylene using H_2O_2 as oxidant with high EO selectivity under mild reaction conditions (35 °C, 50 bars) where CO_2 formation as byproduct is avoided. Further, the observed epoxidation activity [30-800 mg EO/(g metal)/h] is of the same order of magnitude as that of the conventional Ag-based catalytic process that operates under harsh conditions where substrate/product burning cannot be avoided. Our results suggest that framework-incorporated metal species are significantly more active for epoxidation compared to the extra-framework metal oxide species. Indeed, neat metal oxide species show little if any epoxidation activity at similar operating conditions. However, the framework incorporation of the metals introduces Lewis acidity that gives rise to undesired reactions

including solvolysis that result in gradual metal leaching and H₂O₂ decomposition. These mechanistic insights pave the way for developing practically viable epoxidation catalysts in which metal leaching and H₂O₂ decomposition are either minimized or totally avoided.

Acknowledgement

This research was supported partially with funds from National Science Foundation Accelerating Innovation Research Grant (IIP-1127765).

References

1. M. Ghanta, B. Subramaniam, H. J. Lee, and D. H. Busch, *AIChE J.*, 2013, **59**, 180–187.
2. M. O. Ozbek and R. A. van Santen, *Catal. Lett.*, 2013, **143**, 131–141.
3. M. V. Badani, J. R. Monnier, and M. A. Vannice, *J. Catal.*, 2002, **206**, 29–39.
4. J. C. Dellamorte, J. Lauterbach, and M. A. Barteau, *Ind. Eng. Chem. Res.*, 2009, **48**, 5943–5953.
5. M. Ghanta, Doctoral dissertation, University of Kansas, 2012
6. B. Subramaniam, D. H. Busch, H. J. Lee, M. Ghanta, T-P. Shi. “Process for selective oxidation of olefins to epoxides. US Patent 8,080,677 B2, Issued Dec 20, 2011.
7. M. Ghanta, T. Ruddy, D. Fahey, D. Busch, and B. Subramaniam, *Ind. Eng. Chem. Res.*, 2013, **52**, 18–29.
8. B. Subramaniam and G. R. Akien, *Current Opinion in Chemical Engineering*, 2012, **1**, 336–341.
9. D. Hoegaerts, B. F. Sels, D. E. de Vos, F. Verpoort, and P. A. Jacobs, *Catal. Today*, 2000, **60**, 209–218.
10. I. Nowak, B. Kilos, M. Ziolk, and A. Lewandowska, *Catal. Today*, 2003, **78**, 487–498.
11. H. Y. Wu, X. L. Zhang, C. Y. Yang, X. Chen, and X. C. Zheng, *Appl. Surf. Sci.*, 2013, **270**, 590–595.
12. J. M. R. Gallo, I. S. Paulino, and U. Schuchardt, *Appl. Catal. A -Gen.*, 2004, **266**, 223–227.
13. M. Selvaraj, S. Kawi, D. W. Park, and C. S. Ha, *J. Phys. Chem. C*, 2009, **113**, 7743–7749.
14. J. Y. Tang, L. Wang, G. Liu, Y. Liu, Y. Z. Hou, W. X. Zhang, M. J. Jia, and W. R. Thiel, *J. Mol. Catal. -Chem.*, 2009, **313**, 31–37.

15. C. Tiozzo, C. Bisio, F. Carniato, L. Marchese, A. Gallo, N. Ravasio, R. Psaro, and M. Guidotti, *Eur. J. Lipid Sci. Technol.*, 2013, **115**, 86–93.
16. E. Poli, J. M. Clacens, J. Barrault, and Y. Pouilloux, *Catal. Today*, 2009, **140**, 19–22.
17. A. Ramanathan, B. Subramaniam, D. Badloe, U. Hanefeld, and R. Maheswari, *J. Porous Mater.*, 2012, **19**, 961–968.
18. A. Ramanathan, R. Maheswari, D. H. Barich, and B. Subramaniam, *Microporous Mesoporous Mater.*, 2014, **190**, 240–247.
19. B. Subramaniam, A. Ramanathan, M. Ghanta, W. Yan. “Alkylene epoxidation with mesoporous catalysts. WO2014004768 A2, Published Jan 3, 2014.
20. T. W. Kim, F. Kleitz, B. Paul, and R. Ryoo, *J. Am. Chem. Soc.*, 2005, **127**, 7601–7610.
21. F. Kleitz, D. Liu, G. M. Anilkumar, I.-S. Park, L. A. Solovyov, A. N. Shmakov, and R. Ryoo, *J. Phys. Chem. B*, 2003, **107**, 14296–14300.
22. J. E. Buffum, R. M. Kowaleski, W. H. Gerdes, "Ethylene oxide catalyst" *US Patent*. 5145824 A, Issued Sep 8, 1992.
23. H. S. Fogler, *Elements of chemical reaction engineering*, Prentice-Hall, 1992.
24. A. Ramanathan, B. Subramaniam, R. Maheswari, and U. Hanefeld, *Microporous Mesoporous Mater.*, 2013, **167**, 207–212.
25. B. Kilos, M. Aouine, I. Nowak, M. Ziolek, and J. C. Volta, *J. Catal.*, 2004, **224**, 314–325.
26. R. A. Sheldon, M. Wallau, I. W. C. E. Arends, and U. Schuchardt, *Acc. Chem. Res.*, 1998, **31**, 485–493.
27. M. C. Capel-Sanchez, J. M. Campos-Martin, J. L. G. Fierro, *Appl. Catal. A-Gen.*, 2003, **246**, 69–77.
28. L. J. Davies, P. McMorna, D. Bethell, P. C. B. Page, F. King, F. E. Hancock, G. J. Hutchings, *J. Mol. Catal. A-Chem*, 2001, 165, 243–247.
29. M. Morey, J. Bryan, S. Schwarz, and G. Stucky, *Chem. Mater.*, 2000, **12**, 3435–3444.
30. M. Ramakrishna Prasad, M. S. Hamdy, G. Mul, E. Bouwman, and E. Drent, *J. Catal.*, 2008, **260**, 288–294.
31. M. V. Cagnoli, S. G. Casuscelli, A. M. Alvarez, J. F. Bengoa, N. G. Gallegos, M. E. Crivello, E. R. Herrero, and S. G. Marchetti, *Sel. Contrib. XIX Ibero Am. Catal. Symp. Sel. Contrib. XIX Ibero Am. Catal. Symp.*, 2005, **107–108**, 397–403.
32. J. M. R. Gallo, H. O. Pastore, and U. Schuchardt, *J. Catal.*, 2006, **243**, 57–63.

Table 1. Physicochemical characteristics of W- and Nb-KIT-6 catalysts^{15,16}

Catalyst ^a	M wt %	S _{BET} ^b (m ² /g)	V _{p, BJH} ^d (cm ³ /g)	d _{p, BJH} ^c (nm)	NH ₃ mmol/g
W-KIT-6 (10)	17.9	625	1.09	6.9	0.30
W-KIT-6 (20)	9.4	778	1.23	6.7	0.33
W-KIT-6 (40)	5.7	832	1.29	6.3	0.26
W-KIT-6 (100)	2.2	927	1.44	6.4	0.12
Nb-KIT-6(10)	13.4	804	1.01	8.5	0.34
Nb-KIT-6(20)	7.2	926	1.16	8.5	0.23
Nb-KIT-6(40)	3.7	991	1.2	8.5	0.15
Nb-KIT-6(100)	1.5	997	1.35	8.5	0.11

^aThe number in the parenthesis represents molar Si/M ratio, ^bS_{BET}=Specific surface area, ^cV_{p, BJH}=Pore volume, ^dd_{p, BJH}=Pore diameter

Table 2. Epoxidation activity of ethylene over W-KIT-6 and Nb-KIT-6 catalysts [Reaction conditions: MeOH = 624 mmol, H₂O₂=118 mmol, AN = 4.9 mmol, catalyst loading = 500 mg, T = 35 °C, Ethylene P = 50 bar (maintained constant), t = 5 h, 1400 rpm]

#	Catalyst ^a	M wt %	EO TOF (±3%)	S _{EO} % (±3%)	X _{H₂O₂} % (±3%)	U _{H₂O₂} % (±3%)
1	W-KIT-6(10)	17.9	34.4	81.4	10.2	3.6
2	W-KIT-6(20)	9.4	43.4	80.0	6.4	3.9
3	W-KIT-6(40)	5.7	66.5	84.0	6.0	3.5
4	W-KIT-6(100)	2.2	152.6	80.0	4.2	5.0
5	Nb-KIT-6(10)	13.4	234	46.8	17.1	18.8
6	Nb-KIT-6(20)	7.2	340	52.7	17.1	13.1
7	Nb-KIT-6(40)	3.7	513	62.6	17.5	8.4
8	Nb-KIT-6(100)	1.5	794	73.4	11.2	7.1
9	WO ₃	79.3	2.49	91.7	2.5	3.7
10	H ₂ WO ₄	73.6	2.63	100.0	6.4	1.3
11	Na ₂ WO ₄	72.1	10.7	94.4	5.2	5.6
12	Nb ₂ O ₅	69.9	4.38	89.5	4.1	4.0
13	Niobium oxalate	51.4	10.1	90.0	8.8	1.0
14	W-KIT-6(100) ^b	0.57	450	94.1	6.8	2.1
15	W-KIT-6(100) ^c	0.24	298	100.0	3.5	2.4
16	Nb-KIT-6(10) ^b	8.9	284	58.3	8.0	14.0
17	Nb-KIT-6(20) ^b	4.9	372	70.0	6.5	10.4
18	Nb-KIT-6(40) ^b	1.4	844	69.1	4.7	9.8
19	Nb-KIT-6(100) ^b	0.4	1789	59.5	4.7	6.7
20	Nb-KIT-6(40)-B2 ^d	3.3	400	64.7	38.7	3.0
21	Nb-KIT-6(40)-B2 ^e	2.9	328	79.4	12.8	5.3
22	Si-KIT-6 ^f	0	0	0	0	0
23	Nb-KIT-6(10) ^g	13.4	0	0	14.1	0

^aThe number in the parenthesis represents molar Si/M ratio. ^bafter 1st 5 h run, ^c after 2nd 5 h run, ^dfresh batch of Nb-KIT-6(40), ^esilylated Nb-KIT-6(40)-B2, ^fBlank run with KIT-6 support as catalyst, ^gBlank run with no ethylene in the reaction

Table 3. Metal leaching from W-KIT-6 and Nb-KIT-6 catalysts [Reaction conditions: MeOH = 624 mmol, H₂O₂=118 mmol, AN = 4.9 mmol, catalyst loading = 500 mg, T = 35 °C, Ethylene P = 50 bar (maintained constant), t = 5 h, 1400 rpm]

#	Catalyst ^a	Leaching ±5%
1	W-KIT-6(100) ^b	74.1
2	W-KIT-6(100) ^c	89.1
5	Nb-KIT-6(10) ^b	33.7
6	Nb-KIT-6(20) ^b	32.4
7	Nb-KIT-6(40) ^b	61.6
8	Nb-KIT-6(100) ^b	72.4
9	Nb-KIT-6(40)-B2 ^{d,b}	36.1
10	Nb-KIT-6(40)-B2 ^{e,b}	26.4
11	Nb-KIT-6(40)-B2 ^{e,b,f}	9.1
12	W-KIT-6 (100) ^g	24.0
13	W-KIT-6 (100) ^h	100

^aThe number in the parenthesis represents Si/M ratio. ^bafter 1st 5h run, ^c after 2nd 5 h run, ^dcalcined Nb-KIT-6(40)-B2, ^esilylated Nb-KIT-6(40)-B2, ^fSilica leaching from silylated catalyst. ^gBlank run of leaching study, in the presence of methanol only (without H₂O₂ or ethylene). ^hBlank run of leaching study, in the presence of H₂O₂ only (without methanol or ethylene).

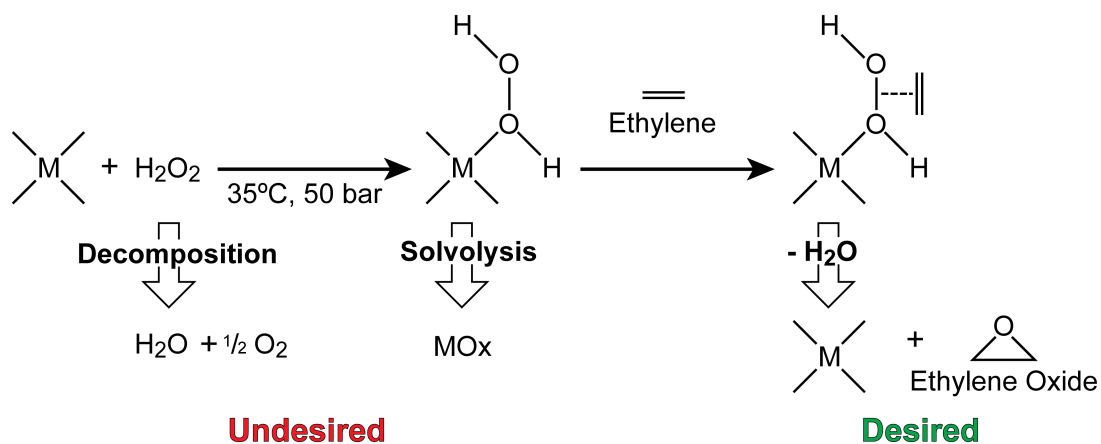
Table 4. Estimates confirming absence of mass transfer limitations*

Mass transfer step	Criterion	Estimated value
Gas-liquid	$\alpha_1 = \frac{R_{EO}}{k_l a C_{H_2O_2}} < 0.1$	$1.83(10^{-4})$
Liquid-solid	$\alpha_2 = \frac{R_{EO}}{k_s a_p C_{H_2O_2}} < 0.1$	$3(10^{-13})$
Intraparticle	$\phi_{exp} = \frac{d_p}{6} \left[\frac{(n+1)\rho_p R_{EO}}{2D_e w C_{H_2O_2}} \right]^{1/2} < 0.2$	$9.5(10^{-4})$

*Details of calculations are shown in Tables S1 and S2 (ESI)

Table 5. Effect of temperature on ethylene epoxidation activity over Nb-KIT-6(20). Reaction conditions: MeOH = 624 mmol, H₂O₂ = 118 mmol, AN = 4.9 mmol, Catalysts = 500 mg, Ethylene P = 50 bar (maintained constant), t = 5 h, 1400 rpm

T °C	EO TOFs (±3%)	S_{EO} % (±3%)	X_{H₂O₂} % (±3%)	U_{H₂O₂} % (±3%)
35	447	76.3	15.1	13.5
40	428	62.9	20.3	11.6
50	438	38.2	36.9	10.8



Scheme 1. Proposed reaction/deactivation mechanism. M denotes either W or Nb, coordinated tetrahedrally within the KIT-6 matrix

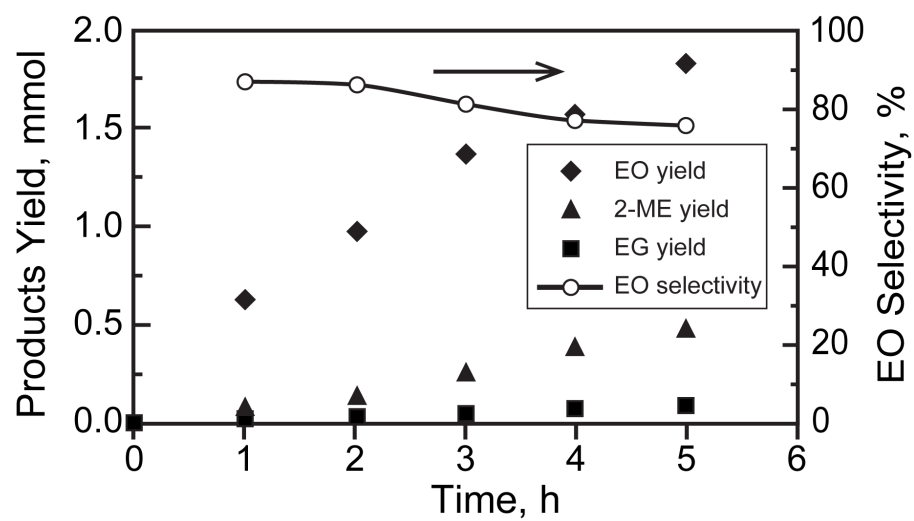


Figure 1. Temporal variations in formation of EO and byproducts over Nb-KIT-6(20) at 35 °C.

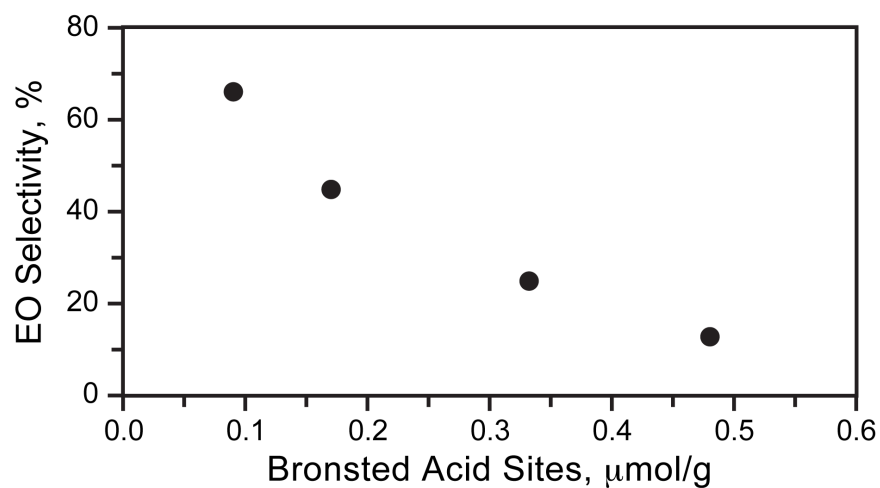


Figure 2. Detrimental effect of Brønsted acid sites on EO selectivity over different Nb-KIT-6 catalysts (Brønsted acidity values taken from Ref. 16). Experimental conditions are the same as those listed in Table 2.